

# THE MODE LOCALIZATION PHENOMENON: VISUAL TEST RESULTS\*

M. Levine- West and M. Salama  
Jet Propulsion Laboratory  
California Institute of Technology  
Pasadena, CA. 91109

## ABSTRACT

The high degree of manufacturing precision required in space structures may make them more susceptible to mode localization. In this demonstration, the mode localization phenomenon is investigated using an existing full scale antenna-like structure having the complexity, manufacturing precision, and dynamic characteristics of space structures. The actual imperfections were measured and incorporated in a numerical model of the structure. The impact of several parameters that provoke the phenomenon were first studied by numerical simulations, then experimentally. The results show excellent agreement, thereby confirming the importance of mode localization in the design of actual space structure.

## I. INTRODUCTION

Many investigations [I-9], have analytically established that the presence of small imperfections in an assembly of nominally identical structural components can drastically alter the expected regular modal behavior of the structure. The phenomenon is known as mode localization (ML), and the origin of its discovery in solid-state physics dates back to the fifties [10,11]. When a mode becomes strongly localized, its modal energy may be confined spatially to only a small number of components of the structural system, instead of being extended throughout the structure had the imperfections not existed. The phenomenon is strongly displayed when the coupling between components is weakest. It is distinguished from the usual ideal behavior by the fact that only very small imperfections in the similitude (or regularity) of the component properties are sufficient to produce disproportionately severe aberrations in modal response.

---

\* The research described herein was performed by the Jet Propulsion Laboratory, California Institute of Technology, under contract with NASA. Funding was provided in part by Dr. A. Das, Air Force Phillips Laboratory, and S. Venneri, NASA office of Aeronautics and Space Technology. The valuable help and discussions with A. Ahmed of JPL, Profs. P. Friedmann and O. Bendiksen of UCLA, and Prof. J. Beck of Caltech are gratefully acknowledged.

Previous investigations have also given insight into understanding the physical phenomenon by demonstrating it on specially designed laboratory experiments with controlled amounts of imperfections and coupling parameters [1,2]. In these experiments, the test articles and scope had to be intentionally simple but revealing. In other experiments [12], observations were made with regard to the effect of small variations in properties on the deviation from ideal mode shapes - although the effects were not attributed at the time to ML. Questions still remained as to: (a) whether the phenomenon can be shown to manifest itself in a non-trivial degree in a realistic structure having the degree of geometric complexity, manufacturing precision, inter-component coupling, and dynamic characteristics of space structures; and (b) what is the predictive accuracy of simple finite element model-based numerical simulation of the phenomenon. These questions provided the motivation for the laboratory investigations reported herein. Space structures such as astronomical telescopes and reflectors must be built to a high degree of precision. But as the manufacturing tolerances are made small, but practically never null, the degree of imperfections may be brought to within the small perturbation domain where localization is most influential. In the present work, the test article is an existing flexible twelve-rib antenna-like structure (Fig. (1)), which was originally designed to simulate a space reflector to be used for demonstrating adaptive control laws, shape control, and model identification experiments [13]. Existing imperfections in the test structure were not altered during testing. But a number of other parameters that can provoke ML, such as inter-rib coupling stiffness and excitation levels, were varied.

The focus of this paper is on the visual demonstration of ML; in the belief that such a demonstration can provide a deeper appreciation of the nature of the phenomenon and how it manifests itself in realistic structures. Extensive descriptions of the test structure, instrumentation used, data acquisition system, analytical theory and results, as well as test procedure and graphical presentation of test results are given in [14].

## II. THE MODE LOCALIZATION PHENOMENON

Previous investigations have shown the effect of small imperfections on the modal response of weakly coupled periodic or cyclic structures. Such structures may include multiple-span beams, trusses and platforms consisting of repeated bays, and antennas consisting of repeated sectors. The analytical studies of Cornwell and Bendiksen of the localization in a large space reflector [3-5] inspired the present experimental investigation. In this section, we give a brief description of the phenomenon and outline qualitatively the impact of the parameters that provoke it.

The modes of a structure assembled in a periodic or cyclic array of nominally identical components cluster in many groups or bands. Within each band, the number of modes is equal to the number of identical components forming the structure. Also within each band, the individual components deform with the same mode shape and magnitude, but with a phasing dictated by the mode number within the band. In general, the first mode of any band is characterized by all components moving in phase, while the last mode

of the band is characterized by all components moving  $180^\circ$  out-of-phase. If the components are hypothetically identical, the modes within each band become degenerate. However, any small imperfections in properties, geometry, or boundary conditions annihilate the modal degeneracy, but spawn pairs of closely spaced modes.

Imperfections can cause certain modes to “localize”. Modes that localize exhibit pronounced deviations from the regular pattern described above, had the structure been perfect. Under certain conditions, very small imperfections can cause the modal deformations to become spatially confined (or localized) to a single component, instead of being extended throughout the entire structure. For the antenna structure in Fig. (1), let  $\phi_i(\mathbf{x})$  designate the modal deformation at location  $\mathbf{x}$  along rib  $i$ . A good measure of the degree of localization is provided by the ratio  $\Lambda_i(\mathbf{x})$ , between the modal deformation of the imperfect structure to the modal deformation of the perfect one, where each of the modes are normalized to unity [3]:

$$\Lambda_i(\mathbf{x}) = \frac{\phi_i(\mathbf{x})_{imperf.}}{\phi_i(\mathbf{x})_{perf.}} \quad (1)$$

A mode is considered localized if  $\Lambda_i(\mathbf{x}) < 0.1$  for all  $\mathbf{x}$  and  $i$ . The more the deformation is confined to a particular component, the stronger is the degree of localization, and the smaller  $\Lambda$  becomes.

A mode does not localize suddenly [9]. The strength of localization depends on a number of parameters. Important among these are the type, amount and mixture of imperfections, the number of components forming the system, the degree of coupling between components, and the level and pattern of exciting forces. The imperfections can be in dynamic properties, geometry, boundary conditions, or any combination thereof. However, the net effect must amount to no more than 5% perturbation in the resultant frequency of vibration in order to clearly distinguish the severe ML behavior from the usual but more benign dynamic behavior.

A useful measure of the degree of coupling between components, the number of components, as well as the modal density within a band has been suggested by Bendiksen [3]. For the  $j$ th band, the modal bandwidth  $\Delta\lambda_j$  is defined by:

$$\Delta\lambda_j = \frac{\omega_{max,j}^2 - \omega_{min,j}^2}{\omega_{min,j}^2} \quad (2)$$

where  $\omega_{max,j}$  and  $\omega_{min,j}$  are the upper and lower frequencies of band  $j$ . For a system of single degrees-of-freedom,  $\Delta\lambda_j$  increases proportional to the coupling stiffness [5]. Weaker inter-component coupling gives rise to narrower bandwidths and therefore, higher modal density within a band. The narrower the bandwidth, the more sensitive to

localization are the modes within it, especially those modes located at the edge of the band [5,9]. It has also been shown numerically that  $\Delta\lambda_j$  decreases with increasing band number  $j$ , and that higher bands are more likely to localize. The degree of ML also increases with increasing number of components in the system. Thus localization is more likely to occur in structures composed of many imperfect components than in ones with the same imperfections but composed of fewer components.

### III. EXPERIMENTS

#### 1. Test Set-up:

The importance of the demonstration reported herein is that it has been implemented on an existing structure which possesses similar dynamical properties and manufacturing tolerances as those of space structures. The first part of the video gives overall and close-up views of the structure. It simulates a space reflector antenna consisting of twelve flexible ribs (0.233 cm thick, 7.62 cm wide, 2.25 m long) which are clamped to a 1.22 m diameter central hub. The ribs are coupled together circumferentially by two rings of constant-force wire-spring assemblies that simulate the coupling effect of an RF reflective mesh used in real antennas. Varying the inter-rib coupling tension is equivalent to varying the wire-spring stiffness. This is implemented by turnbuckle mechanisms that allow inter-rib tensions from 0.56 N to 44.48 N. In the nominal configuration, the wires of the inner ring are tensioned to 4.45 N, and those of the outer ring are tensioned to 2.22 N. To prevent excessive deformation of the ribs due to gravity, two levitator assemblies are used to suspend each rib at two locations so as to minimize the rms gravitational deformations. Each levitator assembly consists of a 15.24 cm diameter ball-bearing pulley and a counter weight that cables around the pulley and attaches to the rib. The ribs are allowed to deform by up to 40.0 cm. In addition to its own weight, each rib carries nine evenly spaced masses along the length (each 33 gin). *still .3*

Each rib can be excited by one of twelve rib-root force voice-coil actuators which react against a mount rigidly clamped to the hub. The ribs can be excited out-of-plane individually, all twelve at a time, or with any combination in between. Phase shifts between the ribs can also be introduced in the excitation forces. The out-of-plane displacements are measured along the ribs at the inner and outer coupling wire locations by twenty-four 12-bit optical encoders which are nested into the twenty-four pulley rotation shafts. The measured displacements are accurate to within 0.254 mm. *still .4*

The data recorded from the twelve force actuators at the rib-roots and the twenty-four optical encoders measuring the displacement time-histories at two points along each rib, are used to identify the modal properties of the structure. The software "MODE-ID" [15], was used to identify the modal frequencies, damping, mode shapes, and Participation factors from the measured displacement response time-histories.

## 2. Numerical Simulations:

To investigate the conditions under which the test structure may be susceptible to localization, a simple finite element model of the structure was constructed, Fig. (2). Each rib was modeled by ten identical beam elements (six d.o.f. per node), and each tension wire was modeled by two purely tensile elements. Each pulley mechanism is modeled as a rigid body whose rotational motion is driven by the pulley rotational inertia and counterweight inertia. The pulley has one rotational d.o.f. which is constrained to correspond to the out-of-plane displacement d.o.f at the rib attachment. Geometric stiffness arises due to the inter-rib tension, which is introduced in the model as enforced change in the wire length. Since the inter-rib coupling could be accurately adjusted using the turnbuckle, no coupling imperfections were assumed in the model. Imperfections in the structural dimensions (e.g. thickness, width of each rib) were measured directly wherever possible. Measured variations in the counterweight masses and inferred rib densities were less than 5%. Since friction and stiction in the pulleys are almost impossible to model, the damping was equivalently incorporated into the inertia of the pulleys. Values of the pulley inertias were adjusted from their nominal values by matching the numerical modal frequencies of each rib to the experimental frequencies obtained by testing the ribs individually without any coupling wires.

Using the model described above, the structure was analyzed in a number of configurations where variations were introduced in the inter-rib coupling tension and in the exciting force patterns and levels. More details are given in [14]. First, a modal analysis of the “perfect” structure (i.e. all ribs identical) was performed with coupling set at the nominal tension of 4.45 N in the inner ring and 2.22 N in the outer ring. The results are summarised in Table (1) for the first 24 modes comprising the first two bands. According to Eq. (1), the width of the first two bands is respectively,  $\Delta\lambda_1 = 1.13$ , and  $\Delta\lambda_2 = 0.052$ . In modes of the first band, all ribs deform in the first cantilever bending mode with a phasing that ranges from  $0^\circ$  to  $180^\circ$ . In modes of the second band, all ribs deform in the second cantilever bending mode with a phasing that ranges from  $0^\circ$  to  $180^\circ$ . According to the ML theory (Sec. II), modes of the second band are more susceptible to localization.

Second, a modal analysis of the structure with the measured imperfections was performed, again with the nominal inter-rib coupling. The resulting frequencies of the first 24 modes are also listed in Table (1). Here the bandwidth of band-1 and band-2 are respectively,  $\Delta\lambda_1 = 1.19$  and  $\Delta\lambda_2 = 0.11$ . In Fig.(3) the first mode of each of band-1, and band-2 is shown, where the solid and dotted lines represent the undeformed and the deformed shapes, respectively. Mode- 1-band-1 show very slight irregularity in rib deformations over the expected uniform umbrella shape, while mode- 1-band-2 shows deformations that are **noticeably** localized in ribs #5 through #12. The numerical results (not shown) also predict strong localization in mode-12-band-2 (the last mode in this band), where the deformation is confined primarily in rib #10. Intermediate modes exhibited only small irregularities.

In addition to the nominal inter-rib coupling tension, other couplings analyzed included: 1/10, 1/4, 1/2 of the nominal coupling, and 2, 3, 4, and 10 times the nominal coupling. Table (2) summarizes the frequencies of selected modes in band-1 and band-2. The following observations emerge from the coupling sensitivity analysis:

- a. The modal bandwidth  $\Delta\lambda_j$  decreases and the structure's susceptibility to ML increases as the band number increases and as the coupling tension decreases. For the reflector structure under consideration, bands with  $\Delta\lambda_j < 0.5$  are not sensitive to ML. Thus, mode-1-band-1 should not be expected to localize, but mode-1-band-2 and higher modes should localize.
- b. As the coupling tension decreases, the coupling stiffness becomes negligible relative to the rib stiffness, and the frequencies within a band become more closely spaced. For coupling tension less than half the nominal, the frequencies within a band become practically indistinguishable. For testing purposes, this means that extracting the modes of the antenna from the time-histories will be more intricate as the coupling is decreased.
- c. Inspection of the mode shapes for 1/10 of the nominal coupling reveals that for band-1, only mode-1 and mode-12 at the edges of the band are found to localize weakly. Although intermediate modes are irregular, they are relatively extended. However, for this same configuration, all modes of band-2 are strongly localized and the deformations are mostly restricted to a single rib. Again, as the inter-rib coupling tension is increased, localization effects decrease. When coupling is increased to 10 times the nominal values, all modes of the first two bands become fully extended. The only difference between the perfect and the imperfect structures is that the modes of the perfect one are degenerate, while those of the imperfect one are well-separated.

### 3. Test Results:

A number of preliminary tests were first performed (not shown in video). These included: ( 1 ) Single uncoupled rib tests to measure and identify the imperfections, monitor the damping in the pulleys, quantify the modal frequencies and damping, and update the numerical model of each rib. (2) Sine-sweep tests to identify the lower and upper bounds of the first two bands for the entire structure in the nominal inter-rib coupling configuration. (3) Sine-dwell tests to select the modes to be examined for ML, select suitable excitation force patterns and magnitudes, and tune the dwelling frequency depending upon the inter-rib coupling level. Descriptions and results of these tests are detailed in [14]. From the numerical simulations and preliminary tests, two modes were targeted to demonstrate the ML phenomenon. These are (a) the first umbrella mode (i.e. mode-1-band-1) where all ribs deform in-phase in the first cantilever bending mode, and (b) the second umbrella mode (i.e. mode-1-band-2) where all ribs deform in-phase in the second cantilever bending mode.

In both cases all ribs were excited sinusoidally in-phase with the same amplitude. Even though this excitation pattern matches the ideal response of the structure the experiments still showed that localization occurred.

a. Localization of the First Umbrella Mode (Mode-1-Band-1):

The first umbrella mode was excited in the nominal coupling configuration with all force actuators tuned in-phase to 0.22 Hz. Modal damping was relatively high, about 2.0%. The response evident in the video shows that localization is weak; only slight deviation from the ideal uniform response is apparent. The same was predicted from the numerical simulations in Sec. III-2. Similar results (not shown) were also found for 1/4 and 3 times the coupling tension. The combination of the relatively large bandwidth ( $\Delta\lambda_1 = 1.19$ ) and high modal damping appear to be responsible for the weak localization of band-1 modes.

still is

b. Localization of The Second Umbrella Mode (Mode-1-Band-2):

As identified from the sine-sweep tests, the second umbrella mode was excited in the nominal coupling configuration with all force actuators tuned in-phase to 1.47 Hz. Modal damping was found to be about 0.7%, and the width of band-2 was predicted to be about 0.11. The video shows that localization is strong in this mode. Instead of the ideal uniform behavior, the deformation is mostly confined to ribs #5 through #9, with predominant motions in ribs #6 and #9. All other ribs have very little elastic motion, and are just moving relatively rigidly along with the base excitation at the hub. Another way to visualize the degree of modal disorder in real-time, is by observing the relative magnitude of the displacement-time histories displayed on the monitor for different ribs. For example, notice in the video that the displacement responses of ribs #1 and #12 are much smaller than ribs #6 and #9.

still is

still is

When the nominal coupling tension was reduced to 1/4 its original value, the frequency of the second umbrella mode increased only slightly (from 1.47 Hz to 1.475 Hz), but the degree of localization increased dramatically. The video shows the modal response confined to ribs #6 and #9, with all other ribs almost stationary. On the monitor, one can observe the much smaller response time-history at ribs #1 and #12 compared to ribs #6 and #9.

still is

still is

Finally, when the inter-rib coupling tension is increased to 3 times the nominal values, the frequency of the same mode decreased from 1.47 Hz to 1.43 Hz and the modal damping increased slightly to 0.8%. But now localization is only marginal. This was also predicted by the simulations

in Sec. III-2. As the video shows, ribs #6 and #9 which were strongly localized under 1/4 coupling, now have approximately the same level of response as the other ribs. still 10, "

Further tests have also shown that the degree of localization is a function of the excitation level. In the last test shown in the video, the second umbrella mode was excited again - but this time at twice the force level of the previous tests. Higher excitation induced non-linear deformations and increased damping due to air drag, and occasional banging of the counterweights against the pulleys. The result was a decreased localization. Interestingly, when the excitation force was decreased to half the original amount, the degree of localization also decreased, apparently due to low level friction and stiction in the pulleys. still .12

#### IV. SIMULATION - TEST CORRELATIONS

To investigate the correlation between the ML observed in the test structure and the predicted behavior, we consider for comparison the results of tests conducted at the original excitation force level of  $0.5N$ . These are judged to be least affected by measurement noise and by non-linear response of the structure and suspension mechanism. We also note that the numerical model did not include damping directly in the dynamic equation of motion, which could have some effect on the prediction of both ML and the response of closely-spaced modes.

(Comparison of the analysis and test frequencies is given in Table (3) for the first two umbrella modes (i.e mode-1-band-1 and mode-1-band-2) for various levels of inter-rib coupling tensions. For the nominal coupling, the frequencies of these two modes match exactly, and they differ by only 2% for mode-1-band-1 and 0.5% for mode-1-band-2 for other coupling configurations. The excellent correlation is due in part to the method of incorporating the rib properties found from the single-rib tests in the full structural model.

The normalized numerical and experimental shapes for mode-1-band-1 and mode-1-band-2 at nominal coupling are compared in Fig. (4). Minor discrepancies between the numerical and experimental mode shapes arose when the modes were spaced less than 0.01 Hz apart, which is also the spectral accuracy of the measured data. Using modal superposition, it was shown [14] that for band-2, with coupling equal or less than the nominal, MODE-ID identified the sum of the first two closely-spaced modes of the band. Slight differences remain in the amount of deformations observed in the quasi-stationary ribs, typically ribs #10 through #4, and the portion of localized response shared by ribs #6 and #9. The extent of discrepancy, although small, appears to be a function of damping and nonlinearities induced by the excitation force level used in the sine-test.



## V. SUMMARY AND CONCLUSIONS

The experiments described herein validated the mode localization theory on a relatively complex space-like structure, and confirmed that the phenomenon could be predicted using relatively simple numerical model. The video results showed that realistic loosely-coupled, periodic structures, with small imperfections in the quasi-identical components, could suffer large deviations from the expected ideal response. In extreme cases, the modal energy could be confined to a single component and may result in higher stresses than expected. Higher modal bands are more susceptible to localization. Larger amounts of damping, inter-component coupling, and deviation from the perfect similitude among components can reduce the strength of localization. By necessity, however, it is not always possible to retain all these characteristics in large, lightweight precision space structures. This makes them more susceptible to localization. Thus, to limit potential future mission failures, it is important to investigate how ML could be mitigated by passive or active means. The phenomenon should be considered in the design of control systems, and included in the uncertainty modelling of the system's dynamics.

## VI. REFERENCES

1. C.H. Hodges and J. Woodhouse, "Vibration Isolation from Irregularity in a Nearly Periodic Structure: Theory and Measurements". *Journal of the Acoustical Society of America*, Vol. 74, 3, 1983, pp. 894-905.
2. C. Pierre, D.M. Tang, and E.H. Dowell, "Localized Vibrations of Disordered Multispan Beams: Theory and Experiment.", *AIAA Journal*, Vol. 25, 9, Sept. 1987, pp. 1249-1257.
3. O.O. Bendiksen, "Mode Localization Phenomena in Large Space Structures", *AIAA Journal*, Vol. 25, 9, Sept. 1987, pp.1241-1248.
4. P.J. Cornwell and O.O. Bendiksen, "Forced Vibration in Large Space Reflectors with Localized Modes", *Proc. of the 30th AIAA SDM Conf.*, Mobile, AL, April 1989, Paper No. 89-1180-CP.
5. P.J. Cornwell and O.O. Bendiksen, "A Numerical Study of Vibration Localization in Disordered Cyclic Structures", *Proc. of the 30th AIAA SDM Conf.*, Mobile, AL, Apr. 1989, Paper No. 89-1181-CP.
6. P.D. Cha and C. Pierre, "Vibration Localization by Disorder in Assemblies of Mono-Coupled, Multi-Mode Component Systems", *Proc. of the 31st AIAA Dynamics Specialists Conf.*, Long Beach, CA, Apr. 1990, Paper No. 90-1213-CP.

7. S.D. Lust, P.P. Friedmann, and O.O. Bendiksen, "Mode Localization in Multi-Span Beams", Proc. of the 31st AIAA Dynamics Specialists Conf., Long Beach, CA, Apr. 1990, Paper No. 90-1214-CP.
8. S.D. Lust, P.P. Friedmann, and O.O. Bendiksen, "Free and Forced Response of Nearly Periodic Multi-Span Beams and Multi-Bay Trusses". Proc. of the 32nd AIAA SDM Conf., Baltimore, MD, Apr. 1991, Paper No. 91-0999-CP.
9. M.B. Levine-West and M.A. Salama, "Mode Localization Experiments on a Ribbed Antenna", Proc. of the 33rd AIAA SDM Conf., Dallas, TX, Apr. 1992, Paper No. 92-2453-CP.
10. E.W. Montroll and R.B. Potts, "Effect of Defects on Lattice Vibrations", Physical Review, Vol. 100, 1955, pp. 525-543.
11. P.W. Anderson, "Absence of Diffusion in Certain Random Lattices", Physical Review, Vol. 109, 1958, pp. 1492-1505.
12. R.R. Craig, Jr., Y.T. Chung, and M.A. Blair, "Modal Vector Estimation for Closely-Spaced Frequency Modes", Proc. of the 3rd International Modal Analysis Conf., Orlando, FL, 1985.
13. H.C. Vivian et al., "Flexible Structure Control Laboratory Development and Technology Demonstration", JPL Publication 88-29, Oct. 1989.
14. M.B. Levine and M.A. Salama, "Experimental Investigation of the Mode Localization Phenomenon", JPL Internal Report D-8767, Sept. 1991.
15. J.L. Beck, "Statistical System Identification of Structures", Proc. ASCE International Conf. on Structural Safety and Reliability, San Francisco, CA, Aug. 1989.

Mode #	Modal Frequency (Hz)			
	Band-1		Band-2	
	Ideal	Imperfect	Ideal	Imperfect
1	0.220	0.216	1.516	1.473
2	0.228	0.224	1.519	1.479
3	0.228	0.225	1.519	1.491
4	0.249	0.246	1.526	1.493
5	0.249	0.247	1.526	1.499
6	0.275	0.270	1.536	1.503
7	0.275	0.273	1.536	1.506
8	0.299	0.294	1.545	1.509
9	0.299	0.296	1.545	1.518
10	0.315	0.309	1.552	1.525
LL-II	0.315	0.309	1.552	1.534
12	0.321	0.320	1.555	1.555

Table 1. Band-1 and Band-2 modal frequencies of the numerical 12-rib antenna model at **nominal** inter-rib coupling with no structural imperfections (all ribs have Rib #1 properties), and with **measured** small imperfections obtained from the single-rib tests.

COUPL'G TENSION	BAND-1 MODE #				BAND-2 MODE #			
	1	2	3	12	1	2	3	12
<b>zero</b>	0.230	0.230	0.230	0.246	1.480	1.487	1.489	1.549
<b>10%</b>	0.230	0.231	0.233	0.252	1.480	1.487	1.490	1.550
25%	0.228	0.231	0.233	0.264	1.480	1.486	1.490	1.550
<b>50%</b>	0.224	0.229	0.231	0.284	1.478	1.483	1.492	1.552
<b>nominal</b>	<b>0.216</b>	<b>0.224</b>	<b>0.225</b>	<b>0.320</b>	1.473	<b>1.479</b>	<b>1.491</b>	<b>1.555</b>
<b>x2</b>	0.196	0.213	0.214	0.377	1.458	1.469	1.476	1.563
x3	0.173	0.200	0.201	0.422	1.442	1.456	1.461	1.573
<b>x4</b>	0.147	0.185	0.186	0.459	1.425	1.441	1.446	1.583
<b>x10</b>	.**	0.095	0.095	0.714	1.317	1.347	1.355	1.725

Table 2. Sensitivity analysis of selected **modal** frequencies (**Hz**) of the 12-rib flexible antenna model with existing structural imperfections (< 4%) as a function of the inter-rib coupling tension. The nominal coupling tension is 4.45 **N** (1.0 **lbf**) at the outer-wire **connection** location and 2.22 **N** (0.5 **lbf**) at the inner-wire **connection** location.

RATIO OF NOMINAL COUPLING	1 <sup>st</sup> UMBRELLA MODE (rib 1 <sup>st</sup> -bending)			2 <sup>nd</sup> UMBRELLA MODE (rib 2 <sup>nd</sup> -bending)		
	F.E.M. MODEL	EXPERIMENT		F.E.M. MODEL	EXPERIMENT	
		ORIG'L	REPEAT		ORIG'L	REPEAT
no wires	0.230	0.235 (1.3%)		1.480	1.490 (0.9%)	
2s %	0.228	0.228 (2.7%)	0.228 (2.6%)	1.480	1.477 (0.8%)	1.475 (0.7%)
nominal	0.216	0.216 (2.6%)	0.216 (4.1%)	1.473	1.472 (0.6%)	1.470 (0.4%)
x 3	0.173	0.159 (1.6%)		1.442	1.434 (0.8%)	

Table 3. Modal **frequencies** (Hz) and damping (%) of the umbrella modes for the first two rib-bending modes. Comparison between the numerical model, **and** the identified results for **the** original and repeated **sine-dwell tests** at 0.50 *N*.

## FIGURE TITLES

Figure 1. 12-rib antenna testbed structure used for ML experiments.

Figure 2. Finite element model of the antenna testbed structure.

Figure 3. Comparison of analysis modes (at nominal coupling) between the perfect structure [(a) mode-1-band-1,  $f=0.228$  Hz, (c) mode-1-band-2,  $f=1.52$  Hz], and the structure with measured imperfections [(b) mode-1-band-1,  $f=0.216$  Hz, (d) mode-1-band-2,  $f=1.47$  Hz].

Figure 4. Comparison between the numerical and experimental normalized rib deformations with nominal coupling and 0.5 N excitations: (a) mode-1-band-1, (b) mode-1-band-2.

Fig 1

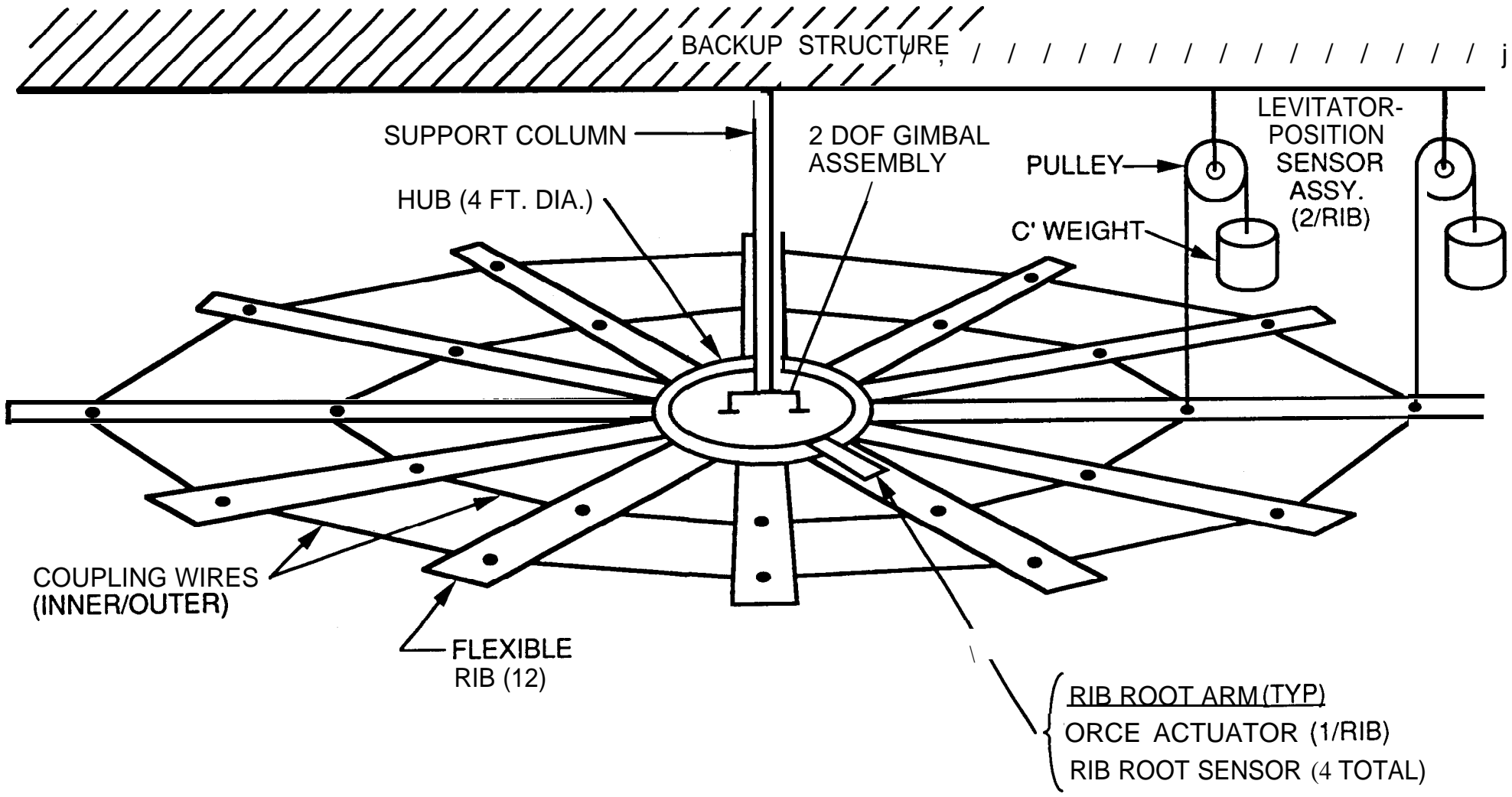


Fig 2

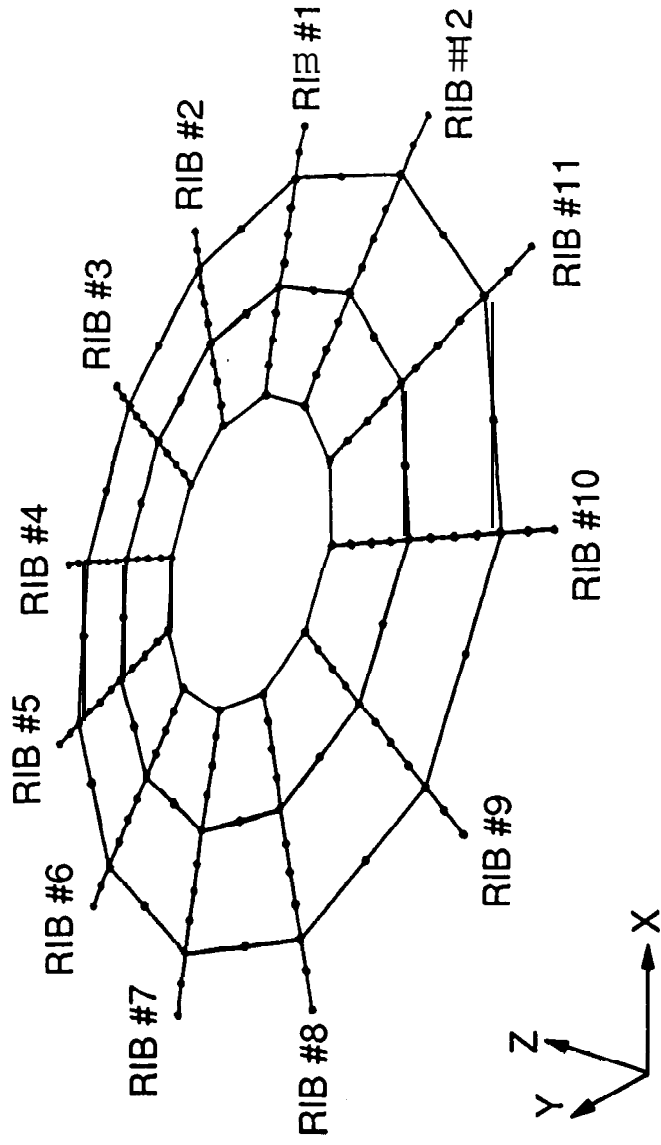
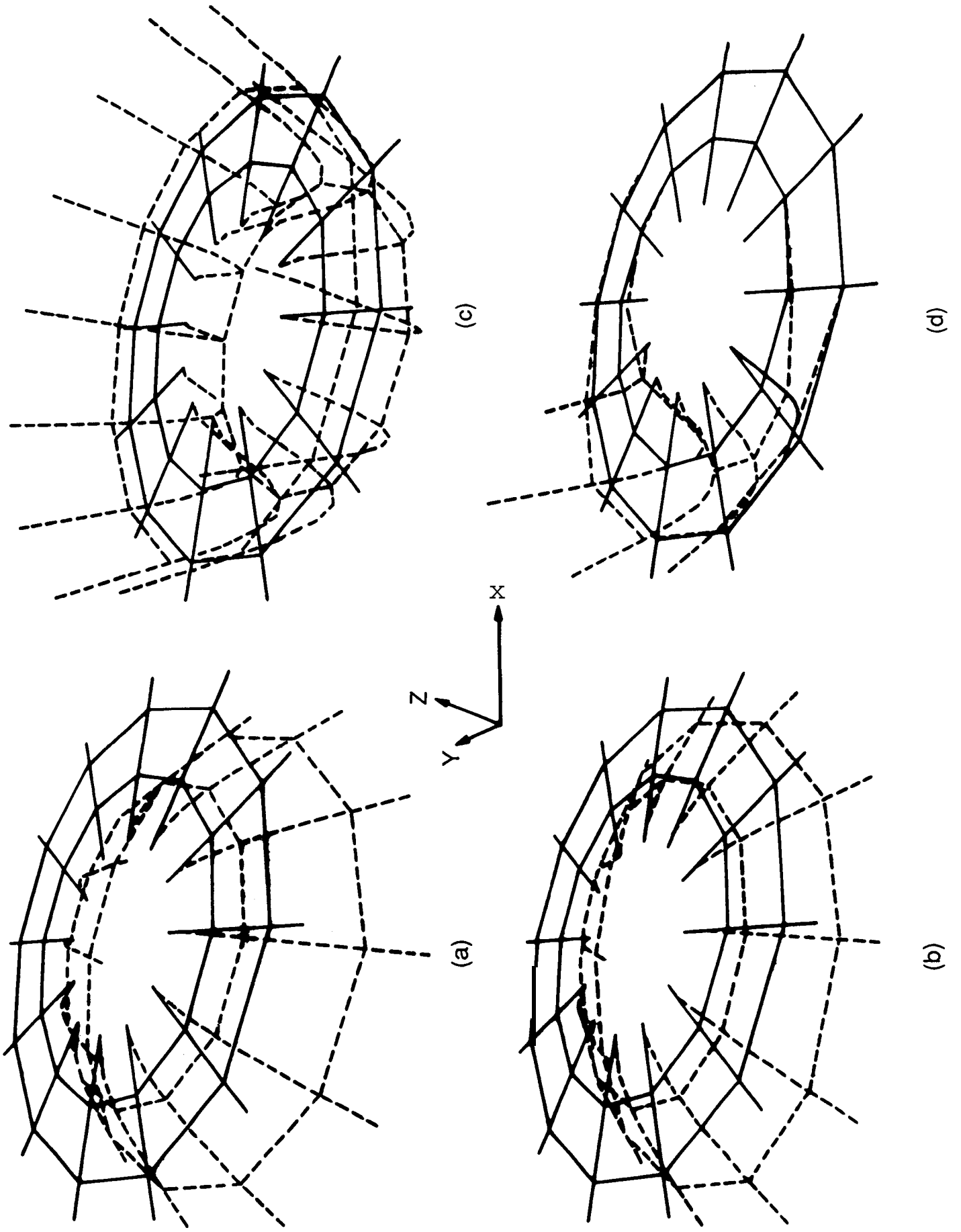
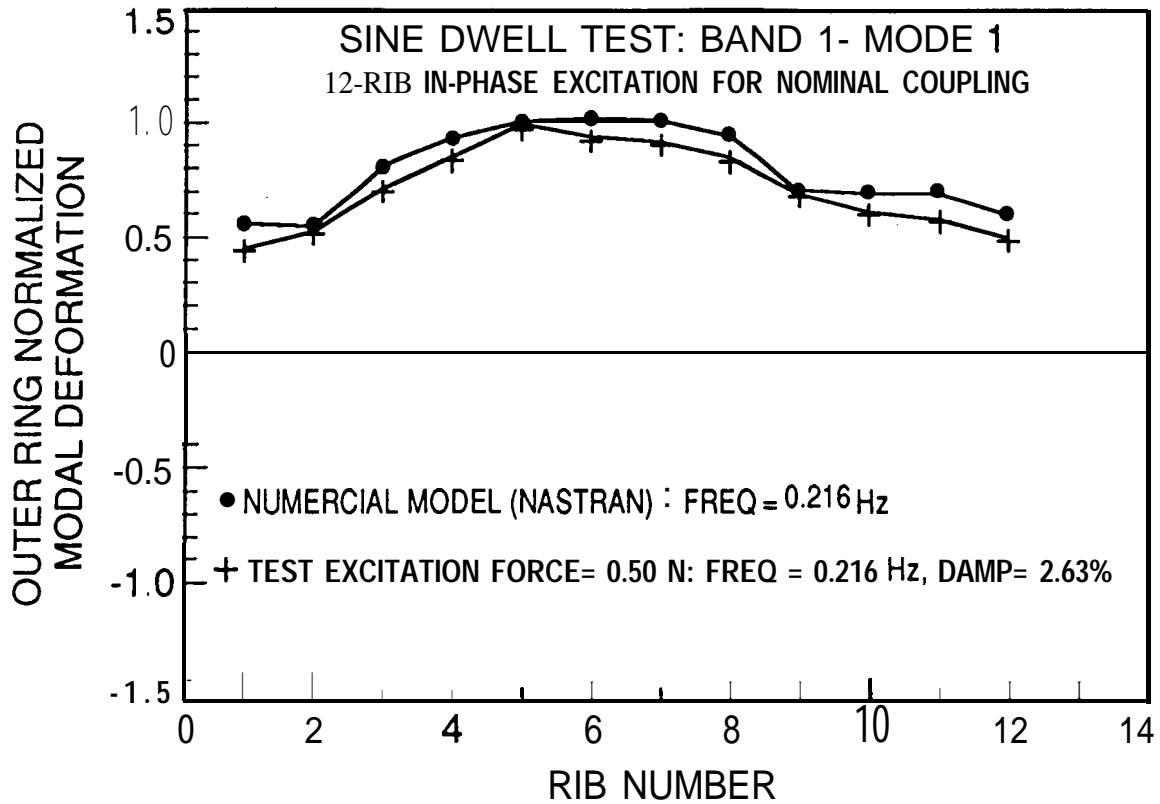


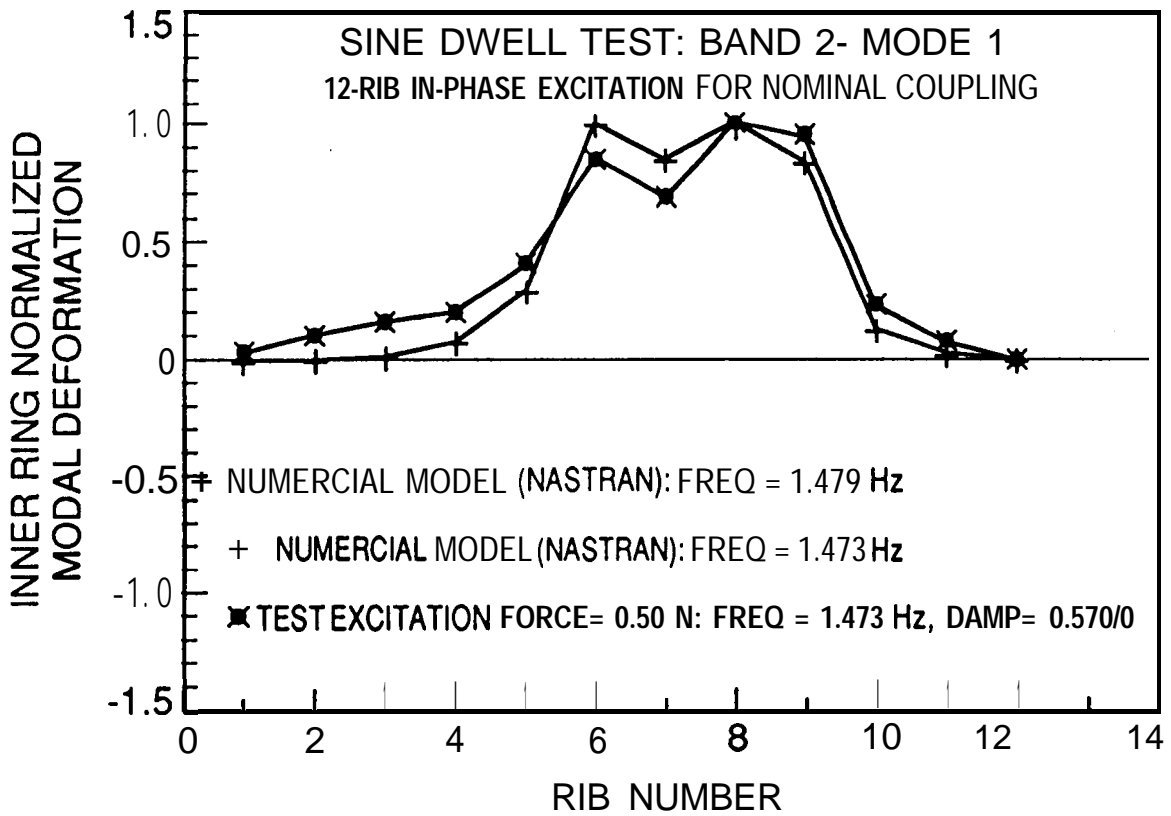


Fig. 3





(a)



(b)

Fig. 4